Supplement of Hydrol. Earth Syst. Sci., 29, 6461–6478, 2025
https://doi.org/10.5194/hess-29-6461-2025-supplement

Hydrology and Earth System Sciences
Open Access
EGU

Supplement of

Impact of rainfall variability on sedimentary and hydropower dynamics in a dam reservoir of southern France

Paul Hazet et al.

Correspondence to: Paul Hazet (paul.hazet@lsce.ipsl.fr)

Contents

Figure S1. Avène lake (left) and Orb dam (right). Credit: A. Foucher, October 2023.

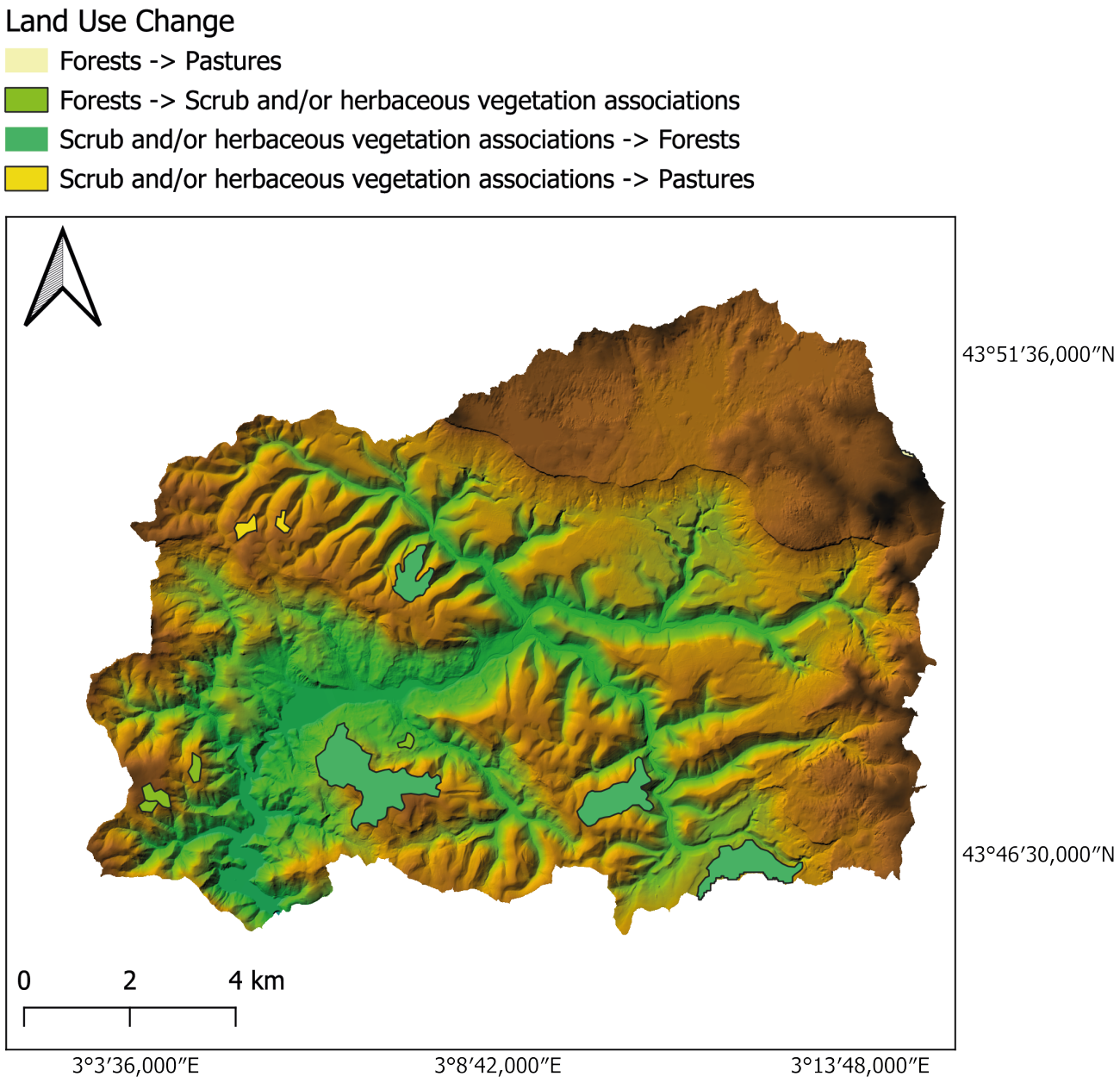

Figure S2. Land use changes (1990-2018) from IGN database showing urbanization patterns.

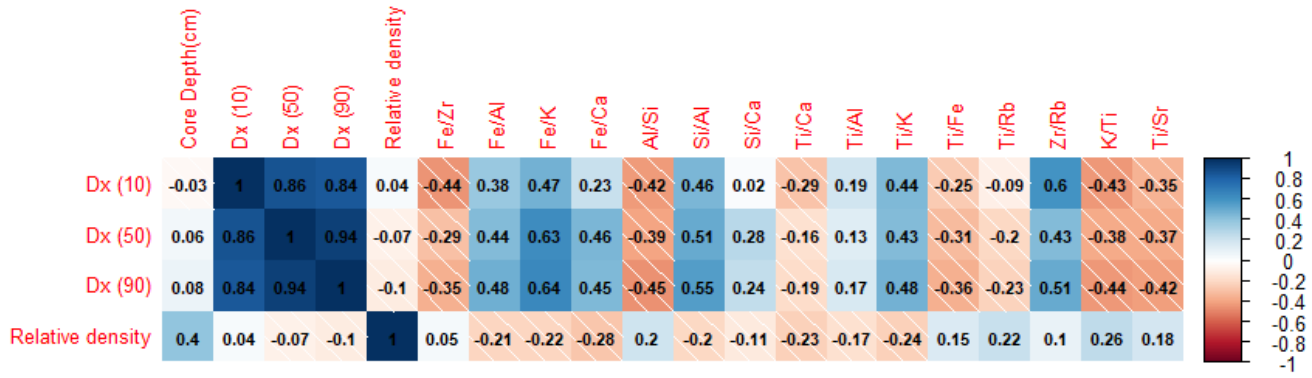

Figure S3. Granulometry and proxies ratio Pearson correlation matrix applied all along the sediment core. Age modelling resulted into approximately 37 years of data comparison. The hatched area corresponds to an anti-correlation between the two elements.

Month	Jan	Feb	Mar	Apr	May	Jun	Jul	Aug	Sep	Oct	Nov	Dec
1976-1997 guideline (mNGF)	428	428.5	429	429.5	430	430	430	430	426	426	427	428
1998-2005 guideline (mNGF)	421.5	422.5	423.5	424	424.3	424.3	424.3	424.3	417.5	418.5	419.5	420.5
Post 2006 guideline (mNGF)	428	428.5	429	429.5	430	430	430	430	426	426	427	428

Table S1. Maximum water level guideline for 1976-1997, 1998-2005 and post 2005 period extracted from BRL report

			Cevenol Average			Unit Average		
Event Number	**Estimated Year**	**Layer (cm)**	**Density**	**Zr/Rb**	**D50-D90**	**Density**	**Zr/Rb**	**D50-D90**
$1^{(3)}$	1987±6.5	92.0 - 92.5	148.7	1.0	3.2-30.4	129.8	0.9	3.0-50.5
$2^{(3)}$	1987±6.4	90.8 - 91.4	148.7	1.1	3.5-41.9	129.8	0.9	3.0-50.5
$3^{(3)}$	1987±6.4	89.5 - 90.0	150.6	0.8	2.7-28.2	129.8	0.9	3.0-50.5
$4^{(3)}$	1988±6.2	87.0 - 87.5	141.1	0.9	3.0-42.7	129.8	0.9	3.0-50.5
$5^{(3)}$	1991±5.7	81.0 - 82.0	152.3	1.0	3.5-107.2	129.8	0.9	3.0-50.5
$6^{(3)}$	1992±5.6	79.2 - 80.0	128.7	1.0	2.9-41.7	129.8	0.9	3.0-50.5
$7^{(3)}$	1993±5.4	75.6 - 76.2	125.7	1.1	3.2-44.3	129.8	0.9	3.0-50.5
$8^{(3)}$	1994±5.2	74.0 - 74.5	122.9	0.9	3.1-54.8	129.8	0.9	3.0-50.5
$9^{(3)}$	1995±5.1	71.5 - 72.0	121.3	0.8	2.6-30.9	129.8	0.9	3.0-50.5
$10^{(3)}$	1995±5.0	70.0 - 70.5	118.4	0.9	2.7-28.4	129.8	0.9	3.0-50.5
$11^{(2)}$	1997±4.8	67.2 - 67.5	128.8	1.0	3.8-55.6	121.0	1.3	4.8-331.5
$12^{(2)}$	1997±4.7	66.0 - 66.7	125.8	1.2	3.9-78.2	121.0	1.3	4.8-331.5
$13^{(2)}$	1998±4.6	63.8 - 64.7	116.1	1.7	4.4-113.3	121.0	1.3	4.8-331.5
$14^{(2)}$	2001±4.0	57.0 - 58.0	131.5	1.5	6.4-864.9	121.0	1.3	4.8-331.5
$15^{(2)}$	2002±3.8	53.0 - 53.9	150.7	1.5	7.3-328.6	121.0	1.3	4.8-331.5
$16^{(2)}$	2005±3.3	47.2 - 47.7	153.8	1.8	4.7-177.5	121.0	1.3	4.8-331.5
$17^{(2)}$	2006±3.1	44.4 - 45.0	138.8	1.2	3.9-126.8	121.0	1.3	4.8-331.5
$18^{(1)}$	2010±2.4	36.2 - 37.2	121.5	1.3	3.2-41.4	119.9	1.0	3.3-53.6
$19^{(1)}$	2015±1.5	25.7 - 26.6	121.0	1.0	3.0-42.6	119.9	1.0	3.3-53.6
$20^{(1)}$	2016±1.3	22.1 - 23.2	128.8	1.3	3.6-58.1	119.9	1.0	3.3-53.6
$21^{(1)}$	2016±1.2	20.7 - 21.5	122.3	1.1	3.3-50.2	119.9	1.0	3.3-53.6
$22^{(1)}$	2018±0.9	16.1 - 16.7	127.0	1.0	3.1-34.8	119.9	1.0	3.3-53.6
$23^{(1)}$	2019±0.7	13.1 - 14.0	126.9	0.9	3.2-34.4	119.9	1.0	3.3-53.6
$24^{(1)}$	2020±0.5	10.7 - 11.2	131.0	1.2	3.1-85.4	119.9	1.0	3.3-53.6
$25^{(1)}$	2021±0.4	9.5 - 9.9	129.9	1.1	3.1-74.1	119.9	1.0	3.3-53.6
$26^{(1)}$	2023-09-12	3.1 - 5.0	109.9	0.9	4.4-81.2	119.9	1.0	3.3-53.6
$27^{(1)}$	2023-09-16	0.0 - 3.0	131.2	1.4	3.5-56.4	119.9	1.0	3.3-53.6

Table S2. Range values of instantaneous events. The average values for Cevenol episodes and stratigraphic (excluding Cevenol episodes values) units are reported for relative density, Zr/Rb ratio, and D50–D90 range. Each estimated age is presented along with its associated uncertainty before age model validation. Age uncertainty was computed using the delta method (first-order error propagation). Units: (1) Unit 1, (2) Unit 2, (3) Unit 3.

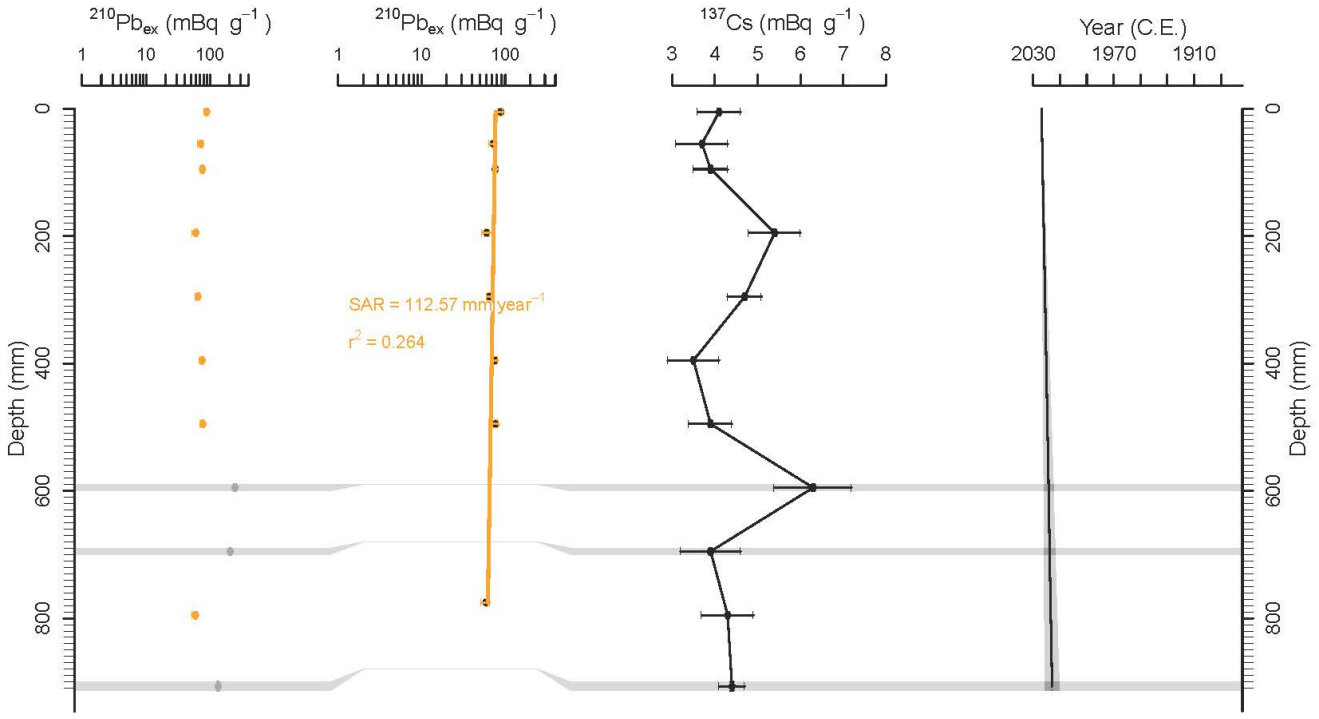

Figure S4. Age model constructed for the ORB01 sediment core using fallout radionuclide activities. From left to right: measured ^{210}Pbex values (orange dots indicate values retained for the model, grey dots excluded from depleted layers); log-linear regression applied to the retained ^{210}Pbex values; ^{137}Cs activity as a function of depth; and estimated deposition years according to the age model. Age uncertainty was computed using the delta method (first-order error propagation).

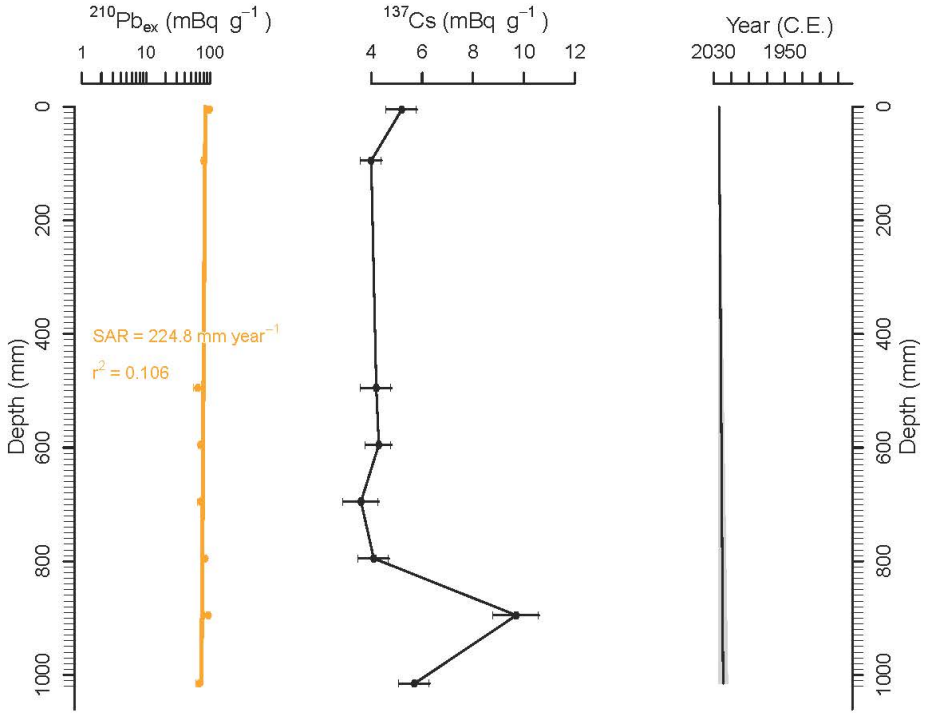

Figure S5. Age model constructed for the ORB06 sediment core using fallout radionuclide activities. From left to right: ; log-linear regression applied to the measured ^{210}Pbex values; ^{137}Cs activity as a function of depth; and estimated deposition years according to the age model. Age uncertainty was computed using the delta method (first-order error propagation).

Date	**Inflow (m^3/s)**	**Date**	**Inflow (m^3/s)**	**Date**	**Inflow (m^3/s)**	**Date**	**Inflow (m^3/s)**
19/10/1969	97.06	05/11/1994	167.39	15/10/1996	101.63	11/12/2002	89.59
17/01/1972	142.28	17/12/1995	139.84	05/12/1996	91.36	27/02/2003	147.50
08/11/1982	264.62	23/01/1996	176.74	07/12/1996	108.54	23/11/2003	96.29
14/11/1984	93.45	29/01/1996	123.30	18/12/1997	241.00	04/12/2003	102.30
27/09/1992	141.73	27/02/1996	105.62	14/11/1999	108.80	30/04/2004	103.19

Table S3. Major flood events, measured in daily volume, recorded at the Monts d'Orb dam between 1965 and 2009, as documented in the BRL report BRl report.

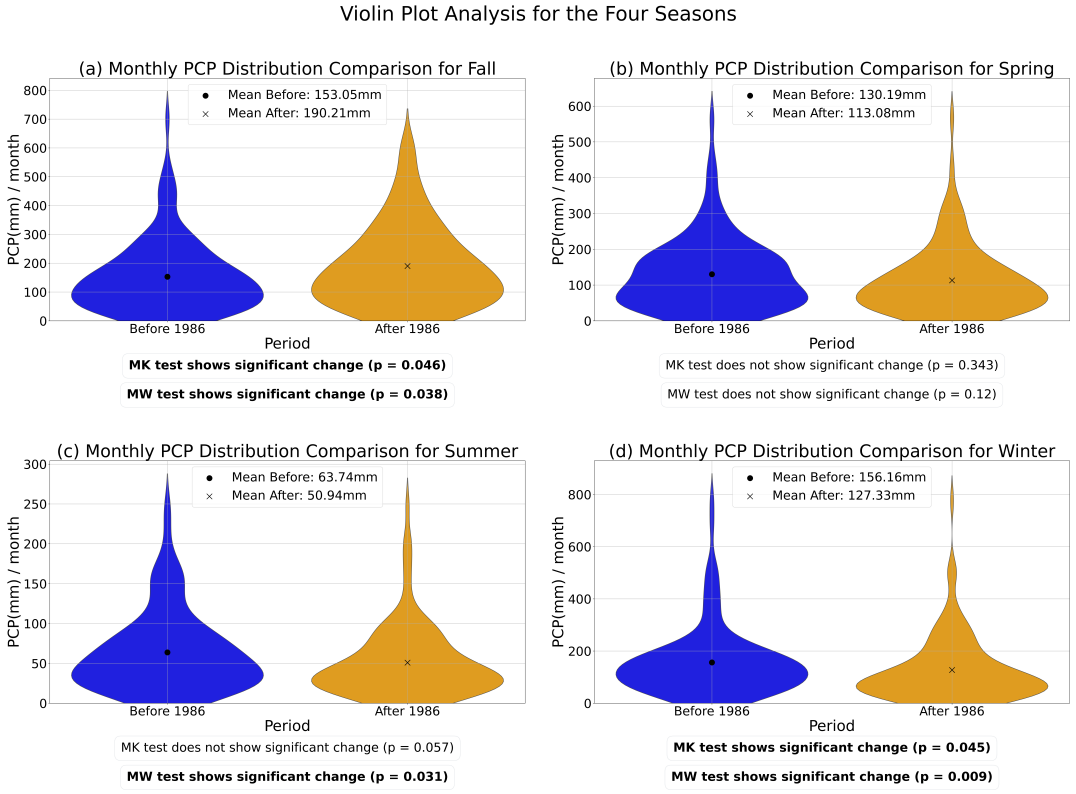

Figure S6. The shift in seasonal cumulative precipitation distribution between the periods 1950–1986 and 1987–2023 was analyzed using the Mann-Whitney test. Additionally, the Mann-Kendall test was applied to detect trends in seasonally aggregated annual precipitation. Statistically significant results are highlighted in bold.

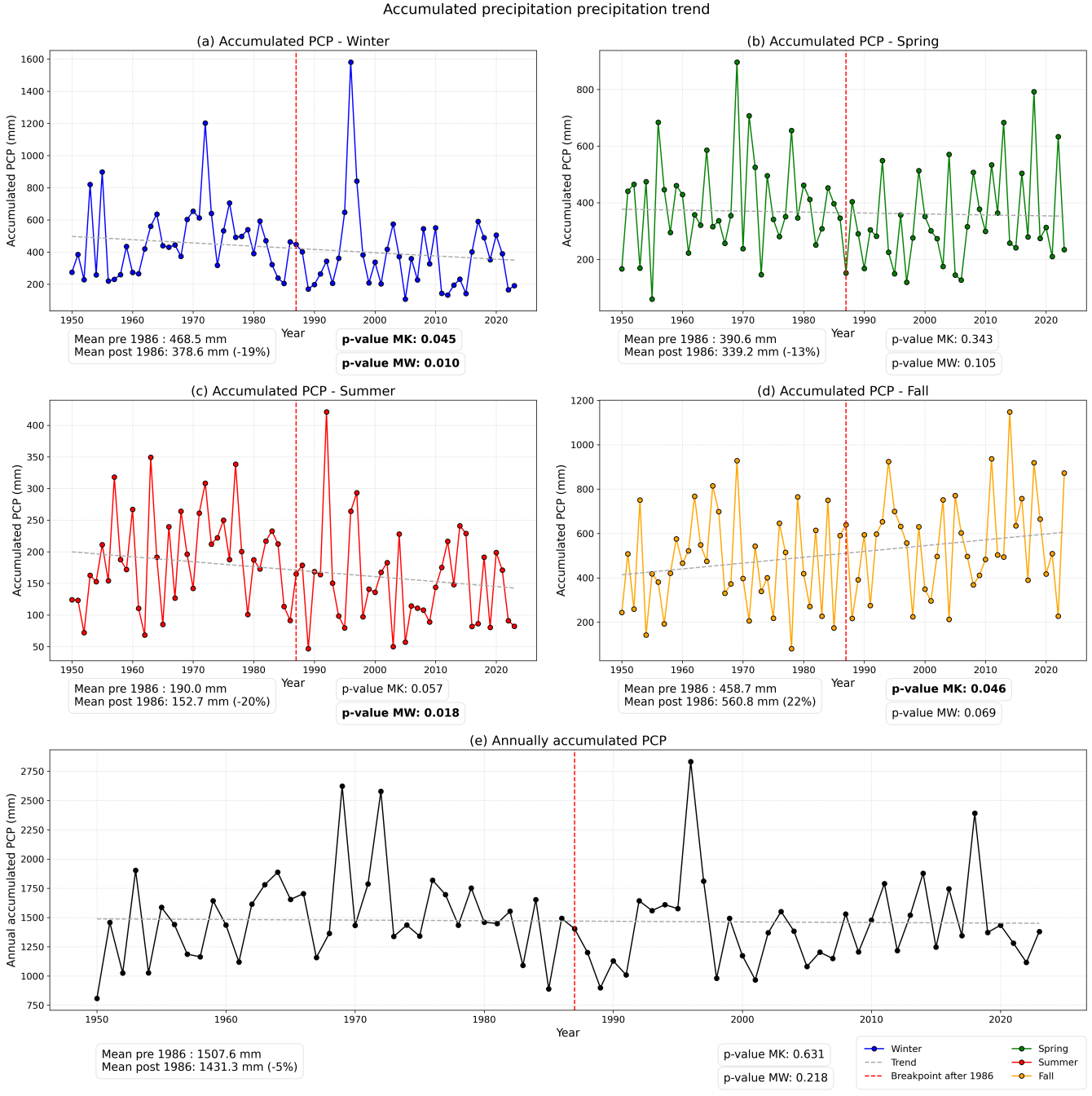

Figure S7. Seasonal and annual precipitation trends. Bold values indicate statistically significant changes (Mann-Whitney U test) and trends (Mann-Kendall test).

Period	Variable	Fall	Spring	Summer	Winter	Annual
Before	avg(mm)	458.7	390.6	190.0	468.5	1507.6
After	avg(mm)	*560.8 (+22%)*	339.2 (-13%)	152.7 (-20%)	***378.6 (-19%)***	1431.3 (-5%)
Before	std(mm/day)	15.0	11.5	7.4	13.1	12.9
After	std(mm/day)	19.2 (+28%)	10.3 (-10%)	5.7 (-23%)	11.5 (-12%)	13.8 (+7%)
Before	100mm E.E	23	12	3	16	54
After	100mm E.E	***43 (+87%)***	9 (-25%)	1 (-67%)	18 (+13%)	71 (+32%)
Before	110mm E.E	17	5	1	13	36
After	110mm E.E	***35 (+106%)***	6 (+20%)	1 (0.0%)	13 (0%)	55 (+53%)
Before	120mm E.E	13	4	1	11	29
After	120mm E.E	***28 (+115%)***	5 (+25%)	0 (-100%)	11 (0%)	44 (+52%)
Before	130mm E.E	11	2	1	6	20
After	130mm E.E	***25 (+127%)***	5 (+150%)	0 (-100%)	8 (+33%)	38 (+90%)
Before	140mm E.E	6	2	0	4	12
After	140mm E.E	***20 (+233%)***	3 (+50%)	0 (+0%)	5 (+25%)	***28 (+133%)***
Before	150mm E.E	3	1	0	3	7
After	150mm E.E	***15 (+400%)***	3 (+200%)	0 (+0%)	4 (+33%)	***22 (214%)***
Before	Max PCP	98.7	73.8	54.7	84.2	125.9
After	Max PCP	***129.5 (+31%)***	67.1 (-9%)	**40.2 (-26%)**	74.7 (-11%)	145.5 (+16%)
Before	$CDD \geq 12$	48	40	66	37	191
After	$CDD \geq 12$	47 (-2%)	46 (+15%)	74 (+12%)	36 (-3%)	203 (+6%)
Before	$CDD \geq 13$	36	33	60	24	153
After	$CDD \geq 13$	39 (+8%)	36 (+9%)	63 (+5%)	**32 (+33%)**	170 (+11%)
Before	$CDD \geq 16$	23	17	46	10	96
After	$CDD \geq 16$	22 (-4%)	21 (+24%)	40 (-13%)	**19 (+90%)**	102 (+6%)
Before	$CDD \geq 20$	17	9	22	2	50
After	$CDD \geq 20$	9 (-47%)	10 (+11%)	21 (-5%)	**7 (+250%)**	47 (-6%)
Before	Max CDD	17.3	17.8	22.8	15.5	25.8
After	Max CDD	18.2 (+5%)	17.7 (-1%)	23.2 (+2%)	18.5 (+20%)	26.7 (+4%)

Table S4. Summary of precipitation changes between the periods 1950-1986 and 1987-2023. The table presents variations in mean precipitation, standard deviation, and the frequency of extreme precipitation events (daily thresholds: 100-150 mm, corresponding to the 99.5th-99.9th percentiles), as well as the occurrence of consecutive dry days (CDD) (thresholds: 12-20 days, corresponding to the 90th-97.5th percentiles). Statistically significant changes are highlighted in bold for the Mann-Whitney test and in italics for the Mann-Kendall test.

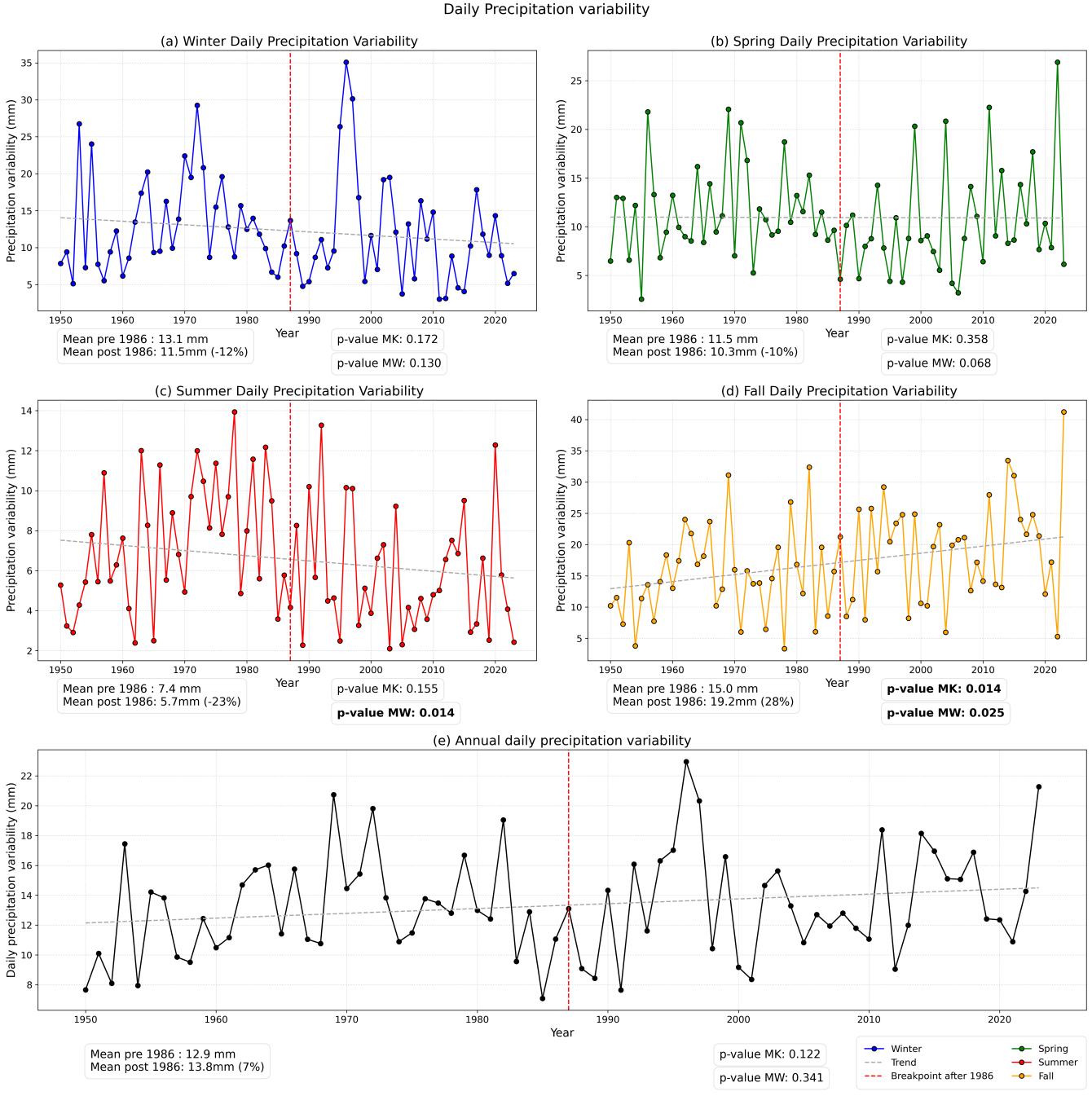

Figure S8. Precipitation variability analysis showing distributional shifts pre- and post-1986 (Mann-Whitney U) and monotonic trends (Mann-Kendall).

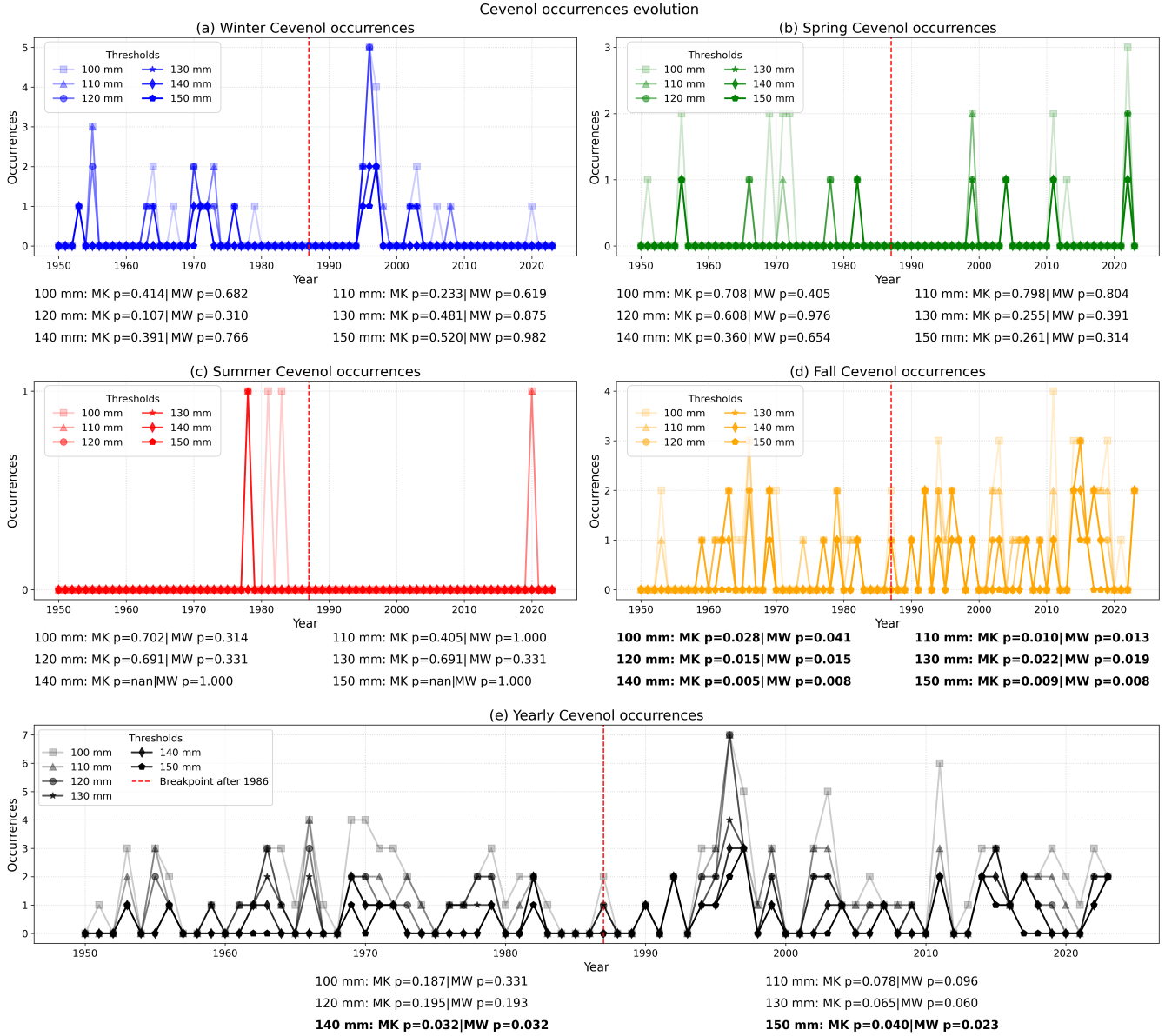

Figure S9. Frequency of Cevenol episodes showing significant increases in autumn (bold values, Mann-Whitney U and Mann-Kendall tests).

Figure S10. Intensity trends of Cevenol rainfall events. Significant results in bold.

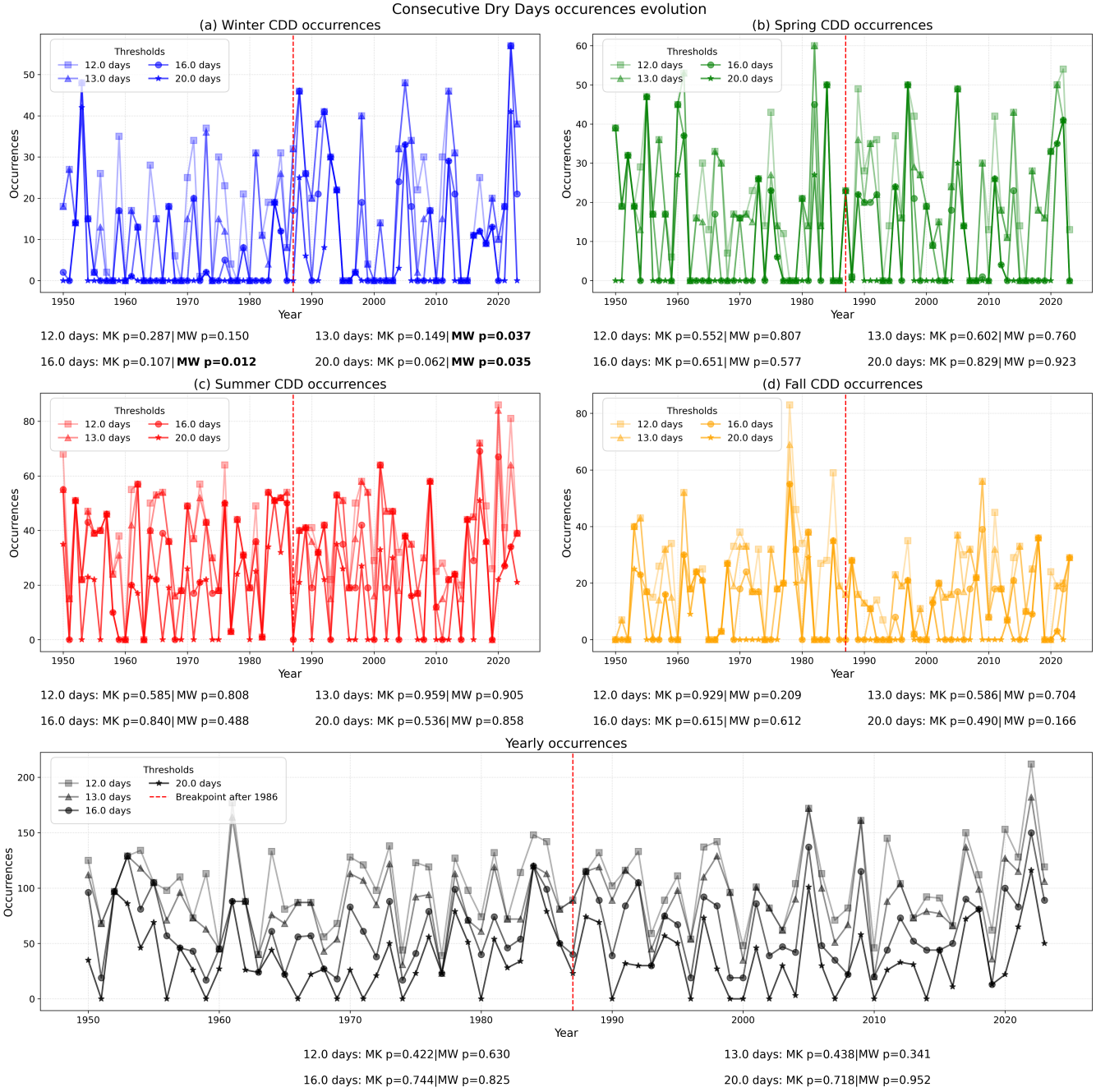

Figure S11. Consecutive Dry Days (CDD) frequency. Significant results in bold.

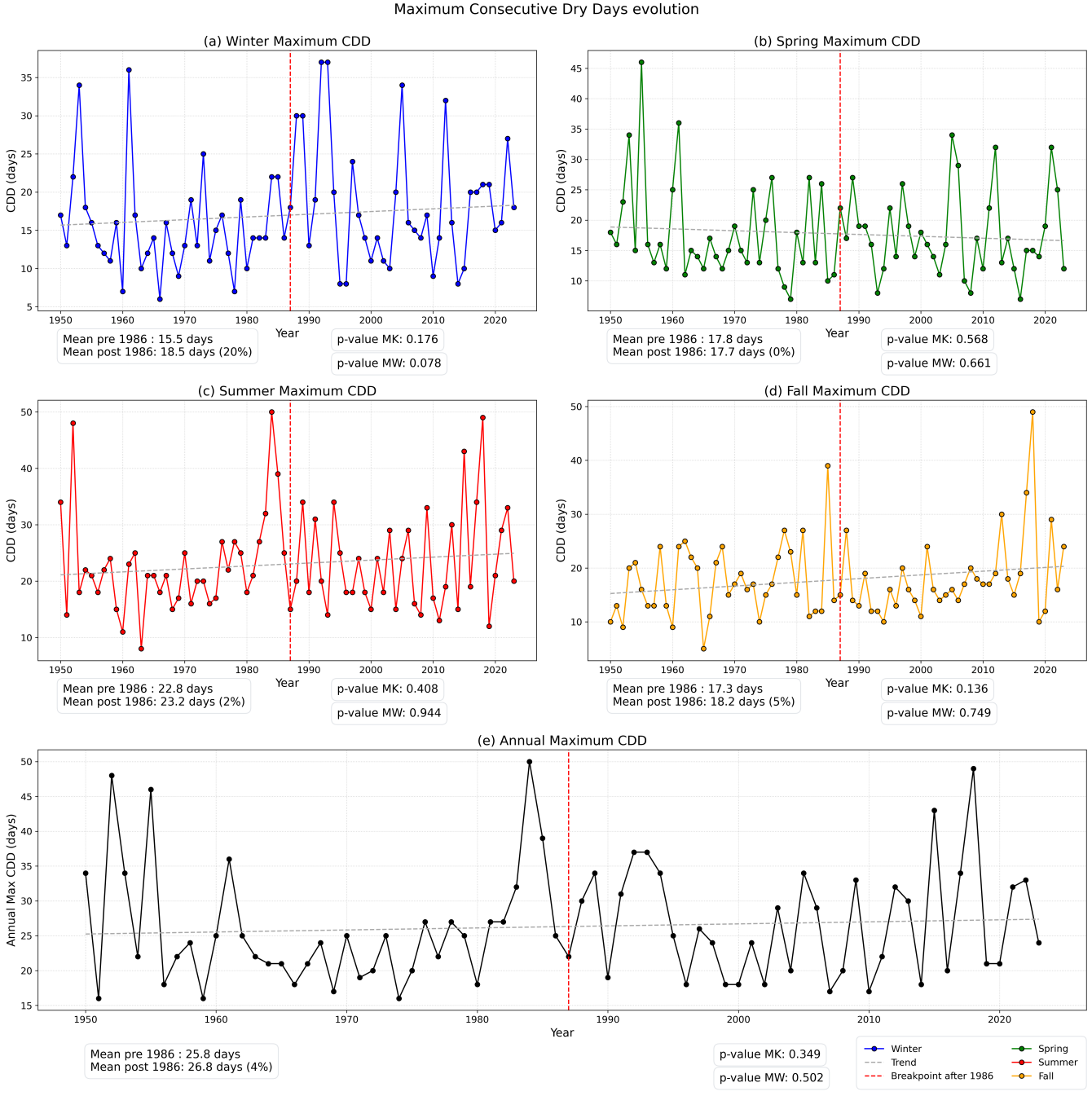

Figure S12. Drought intensity trends. Significance is shown with bold values.

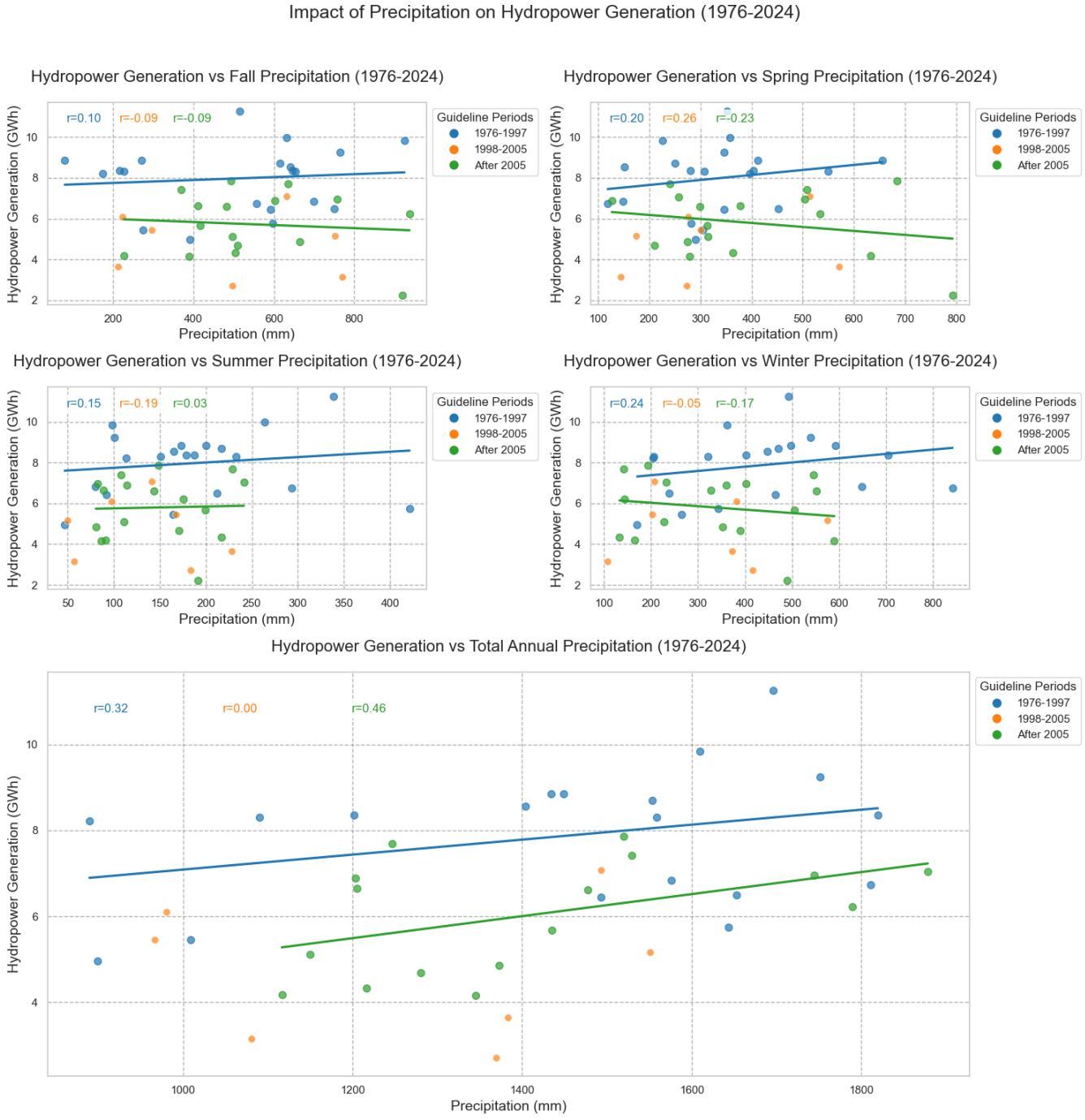

Figure S13. Hydropower production correlations with annual and seasonal precipitation.

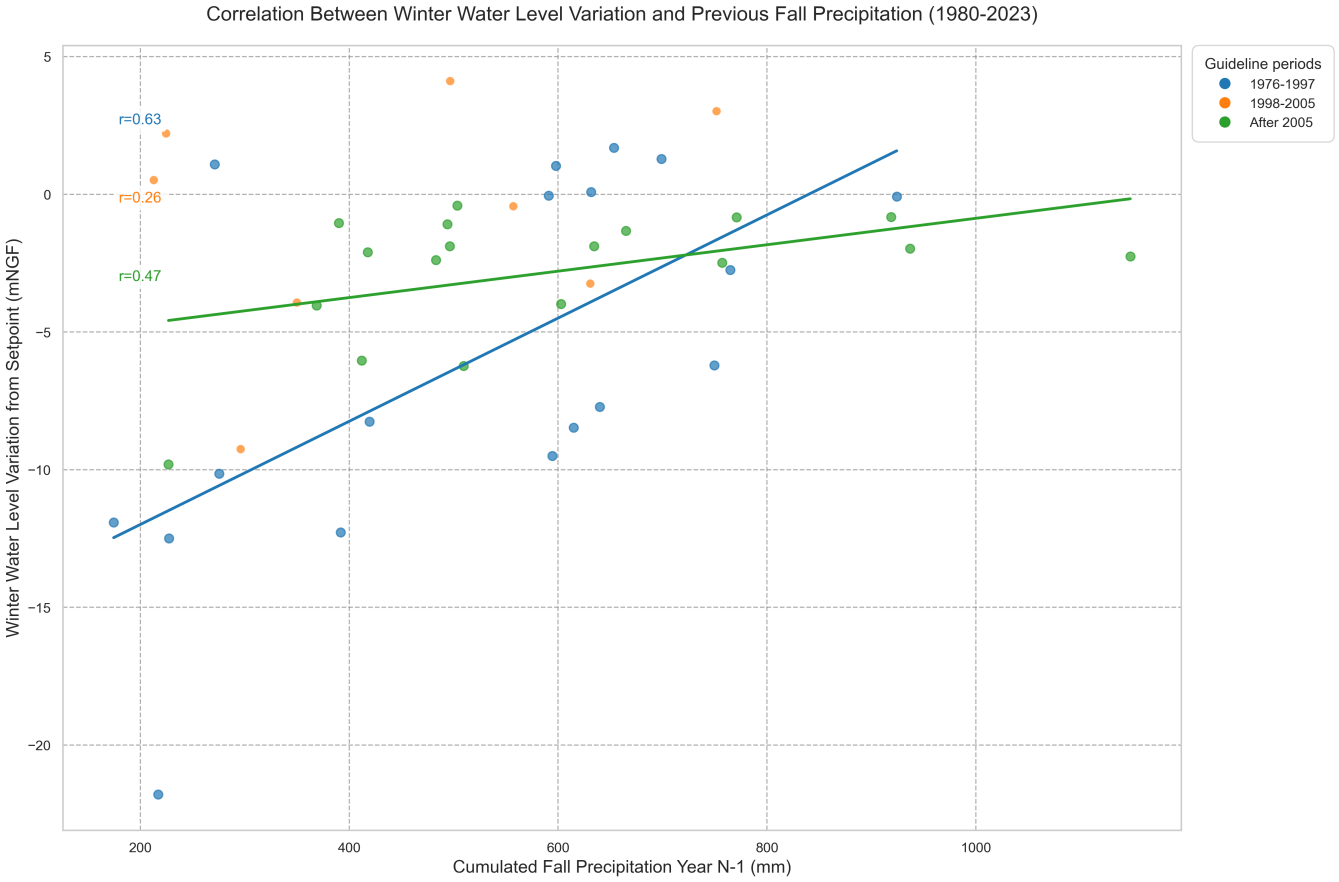

Figure S14. Correlation between average winter water level at year N and precipitation in fall at year N-1.

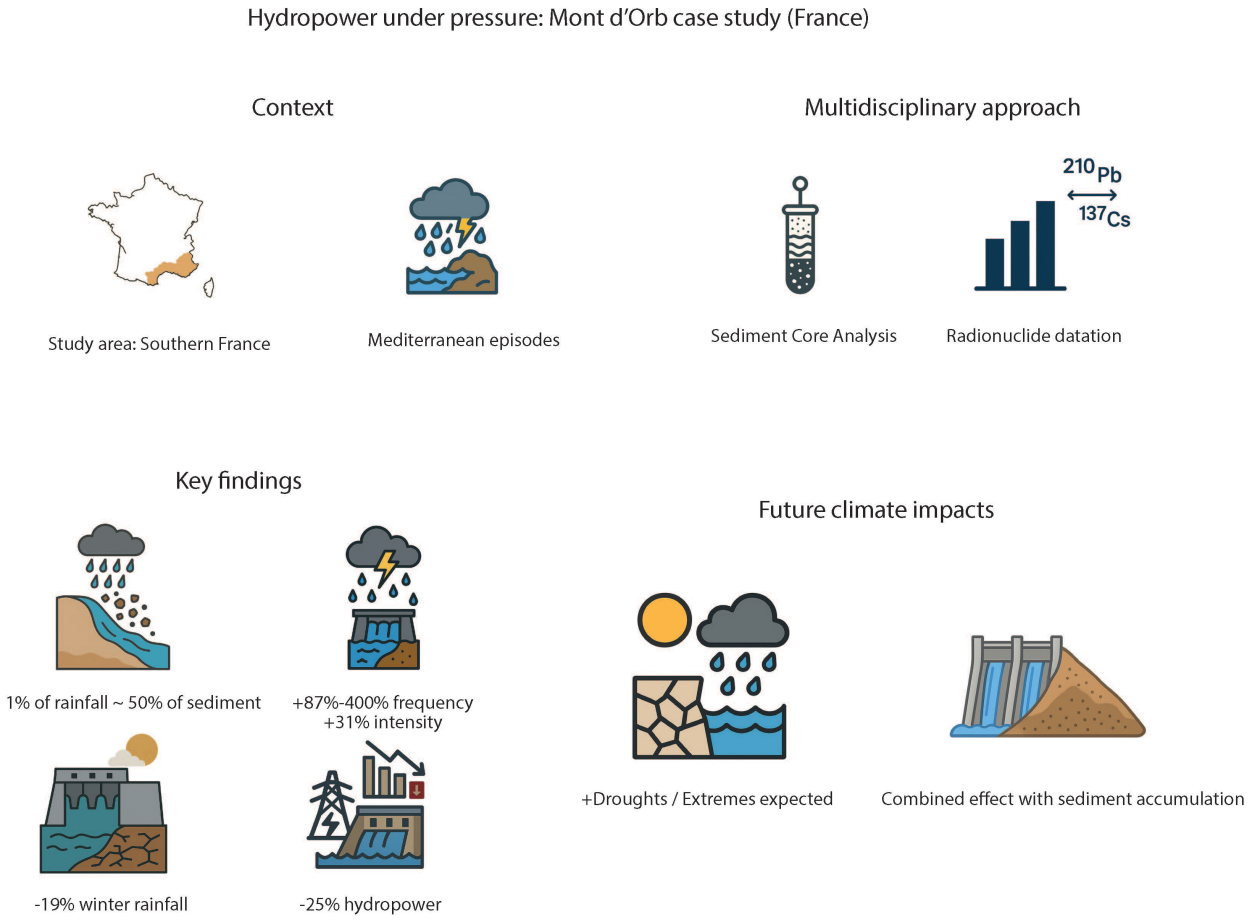

Figure S15. Graphical abstract summarising the key findings and methodological approach of the study.